SLAC-PUB-7924
August 1998

RF loss in and leakage through thin metal film

Xintian Eddie Lin

Submitted to IEEE Transactions on Microwave Theory and Techniques

Stanford Linear Accelerator Center, Stanford University, Stanford, CA 94309

Work supported by Department of Energy contract DE–AC03–76SF00515.

RF loss in and leakage through thin metal film

Xintian Eddie Lin

Abstract— **Traditional RF enclosures are formed by metal bulk material, in which the field decays exponentially over a skin depth $\delta = \sqrt{2/\omega\sigma\mu_0}$. With typical bulk dimension at least one order of magnitude higher than δ, the field outside the metal enclosure is then negligible. The surface resistance R_s presented to the RF field is $1/\sigma\delta$. This article presents analysis of an RF shield formed by thin metal film. We find that a metal thickness Δr of the order of skin depth, can provide an excellent RF shielding due to reflection at the interface. The surface RF loss can be reduced with proper choice of metal thickness, and heating can be reduced. The thin metal film also facilitates cooling on the back of the film via thermal conduction. For a very thin coating, the surface RF loss is inversely proportional to thickness, while inductance is proportional to thickness, and thus it is possible to customize the accelerator beam impedance through careful choice of coating thickness.**

Keywords— **Thin metal film, RF leakage, impedance.**

I. Introduction

METAL coatings are widely used in many applications, one of which is RF shielding. For example, ceramic vacuum chambers are used in accelerator beam monitors, injection kicker and feedback systems, and metal coating is applied to the inner ceramic wall to provide a conduction path and prevent static charge accumulation. Therefore, it is important to characterize the impedance and quantify the RF shielding. Piwinski[1] has analyzed the RF impedance and penetration of metal coating on ceramics through field matching, but did not obtain the minimum surface resistance at $\frac{1}{2}\pi\delta$. Chao[2] has derived the thin film impedance by assuming short circuit boundary condition, which does not apply in this circumstance. Jackson[3] found the impedance of two thin metal layers assuming no RF leakage. Courant and Month[4] also gave the surface impedance of metal film on metal. In this article we analyze the thin film surface impedance and RF leakage assuming outgoing wave boundary condition and also provide the effective impedance presented to a charged particle beam.

II. Surface impedance

To simplify the calculation, we will use the perturbation approach instead of a self-consistent field matching solution. The fields are obtained by first assuming a perfectly conducting boundary, and then applying a small surface impedance as a perturbation. The difference between the perturbation approach and full field matching is of the order of $\frac{1}{2}(R_s/Z_0)(\omega/c)b$; thus for a 2 cm radius copper pipe, at 4.77 GHz, the correction is 5×10^{-5}.

This work is supported by Department of energy under Contract No. DE-AC03-76SF00515.

Xintian E. Lin is with the Stanford Linear Accelerator Center, Stanford University, CA. E-mail: eddie@slac.stanford.edu

A. Thick metal

There are many textbook analyses of RF fields inside metal; however, for convenience and comparison, a brief discussion is provided here.

In the case of a thick metal coating, the fields decay exponentially away from the surface[5]:

$$H_y = H_0 e^{-(1-i)x/\delta} \quad (1)$$
$$E_z = Z_s H_0 e^{-(1-i)x/\delta}, \quad (2)$$

where surface impedance $Z_s = (1-i)\sqrt{\omega\mu_0/2\sigma}$, and x is the normal coordinate. The implicit dependence of $e^{ik_z z - i\omega t}$ on all quantities is suppressed for brevity. The electric current J_z follows from

$$J_z = \sigma E_z = \sigma Z_s H_0 e^{-(1-i)x/\delta}. \quad (3)$$

It is evident from Eq. 3 that the magnitude of fields decay exponentially with penetration into the conductor, and that δ has the significance of the depth where fields drop to $1/e$ of their surface value. Also notice that the phase lags by x/δ radian at depth x into the conductor. Therefore, referenced to the surface, the averaged current flow

$$< J_z >= J_0 e^{-x/\delta} \cos\frac{x}{\delta} \quad (4)$$

reverses the direction at depth $x = \frac{1}{2}\pi\delta$ as shown in Fig. 1.

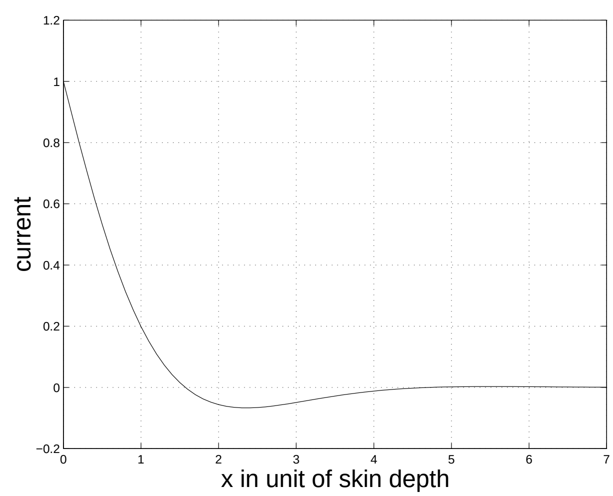

Fig. 1. Current distribution in metal.

B. Thin coating

Without loss of generality, we assume a cylindrical geometry shown in Fig. 2, where regions 1 and 2 are vacuum and metal respectively. Region 3 can be a dielectric or other metal and extends to infinity. We will label quantities with a subscript corresponding to each region unless defined otherwise.

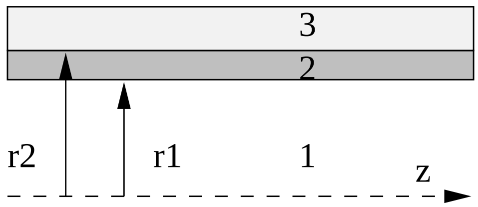

Fig. 2. Metal coating in a cylindrical chamber with inner radius r_1. The coating thickness is $r_2 - r_1$.

When the metal coating is thin compared with skin depth δ_2, the solution of H and E have two terms,

$$H_{2\phi} = ae^{-(1-i)x/\delta} + be^{(1-i)x/\delta} \quad (5)$$

$$E_{2z} = Z_{2c}(ae^{-(1-i)x/\delta} - be^{(1-i)x/\delta}) \quad (6)$$

where a and b represent the outgoing wave and reflected wave amplitude respectively. Here $Z_{2c} = (1-i)\sqrt{\omega\mu_0/2\sigma_2}$ represents the transmission line characteristic impedance of the metal, and $x = r - r_1$. The impedance Z_2 defined at the interface $r = r_2$ can be expressed as

$$Z_2 = Z_{3c} = \frac{k_{3r}}{\omega\epsilon_3}\frac{iH_0^{(1)}(k_{3r}r_2)}{H_0^{(1)\prime}(k_{3r}r_2)}, \quad (7)$$

a result of outgoing radial wave boundary condition in medium 3, where $H_0^{(1)}$ is the Hankel function of the first kind. The radial propagation constant k_{3r} satisfies

$$k_{3r} = \sqrt{(\frac{\omega}{c})^2\epsilon_{3r} - k_z^2}, \quad (8)$$

where ϵ_{3r} is the relative permittivity. When $k_{3r}r_2 \gg 1$, the expression for Z_{3c} reduces to that of a plane wave

$$Z_2 = Z_{3c} = \frac{k_{3r}}{\omega\epsilon_3} = \frac{k_{3r}}{(\omega/c)\epsilon_{3r}}Z_0 \quad (9)$$

For a dielectric the characteristic impedance Z_{3c} is roughly $(\sqrt{\epsilon_{3r}-1}/\epsilon_{3r})Z_0$ assuming $k_z = \omega/c$. It is of the order $Z_0 = 377\Omega$. Meanwhile Z_{2c} for copper at 11 GHz is $0.028(1+i)\ \Omega$. If the material in region 3 is metal, replace ϵ_{3r} by $\epsilon_{3r}(1 + i\sigma_3/\omega\epsilon_3)$. Under the condition $\omega \ll \sigma_3/\epsilon_3$, we recover the expression

$$Z_{3c} = (1-i)\sqrt{\frac{\omega\mu_0}{2\sigma_3}}. \quad (10)$$

From Eq. 5 and 6, one can relate the surface impedance Z_1 at $r = r_1$ with Z_2 by impedance transformation

$$\frac{Z_1}{Z_{2c}} = \frac{(Z_2/Z_{2c})\cos k_{2r}\Delta r - i\sin k_{2r}\Delta r}{\cos k_{2r}\Delta r - i(Z_2/Z_{2c})\sin k_{2r}\Delta r}, \quad (11)$$

where $k_{2r} = (1+i)\sqrt{\omega\mu_0\sigma_2/2}$. In the case that material 2 is a good conductor, and material 3 is a poor conductor, dielectric or even air with $\epsilon_{3r} = 1.0005364$[6], the condition

$$|Z_2/Z_{2c}| \gg 1 \quad (12)$$

holds. We can further simplify Eq. 11 to

$$Z_1/Z_{2c} = i\tan^{-1} k_{2r}\Delta r \quad (13)$$

if

$$|(Z_2/Z_{2c})\sin k_{2r}\Delta r| \gg |\cos k_{2r}\Delta r|, \quad (14)$$

which reduces to

$$\Delta r \gg \frac{\epsilon_{3r}}{\sqrt{\epsilon_{3r}-1}Z_0\sigma_2} \quad (15)$$

for dielectric or

$$\frac{\Delta r}{\delta_2} \gg \sqrt{\frac{\sigma_3}{\sigma_2}} \quad (16)$$

for metal in region 3.

With $\epsilon_{3r} = 5.5$ and $\sigma_2 = 5.8e7\ (\Omega m)^{-1}$ for copper film, Eq. 15 requires $\Delta r \gg 1.2\dot{A}$. In the case of copper film on stainless steel with $\sigma_3 = 0.02\sigma_2$, Eq. 16 requires $\Delta r \gg 0.14\delta_2$.

Eq. 13 can be understood physically from the open circuit boundary condition at $r = r_2$ as Eq. 12 suggests. Chao[2] has derived the thin metal film impedance under the closed circuit boundary condition at $r = r_2$, which does not apply in this circumstance.

In a numerical example of $\epsilon_{3r} = 5.5$ and $k_z = 0.77\omega/c$, the value of Z_1 from Eq. 11 is plotted in Fig. 3. The real

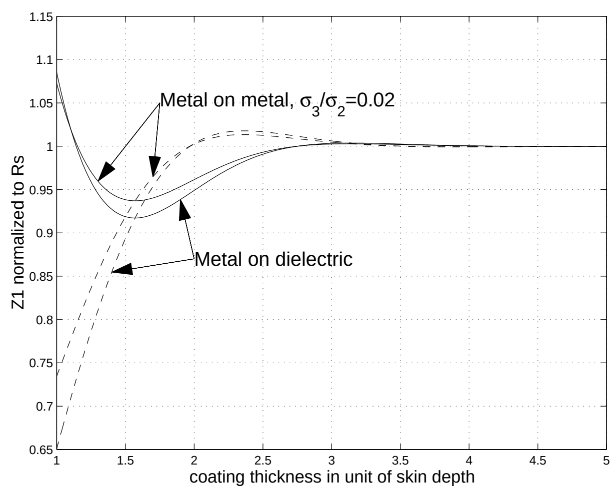

Fig. 3. Surface resistance of a thin metal film as a function of film thickness. The solid lines represent $\Re(Z_1)/R_s$, and the dashed lines represent $-\Im(Z_1)/R_s$. The coating is chosen to be copper and substrate is dielectric with $\epsilon_{3r} = 5.5$ or stainless steel.

part of Z_1, plotted as solid line, exhibits a minimum about $0.92R_s$ at $\Delta r = 1.57\delta_2 \approx \frac{1}{2}\pi\delta_2$. And as expected, when Δr goes to infinity, it approaches R_s. A similar behavior for copper film on stainless steel are shown in the plot too.

Recall that in thick conductor, there are current flowing in the opposite direction at depth greater than $\frac{1}{2}\pi\delta_2$ due to the phase lag. The reduction of the surface loss of a thin film about $\frac{1}{2}\pi\delta_2$ thick is a direct result of eliminating inverse current flow in the conductor. Therefore, the average current density near the conductor surface is reduced. Fig. 4 illustrates the distribution of amplitude and phase

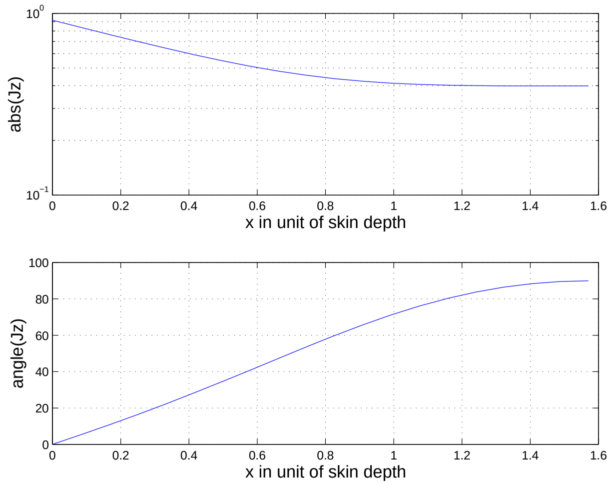

Fig. 4. The amplitude and phase of the electric field in the conductor. The metal film thickness is $\frac{1}{2}\pi\delta_2$.

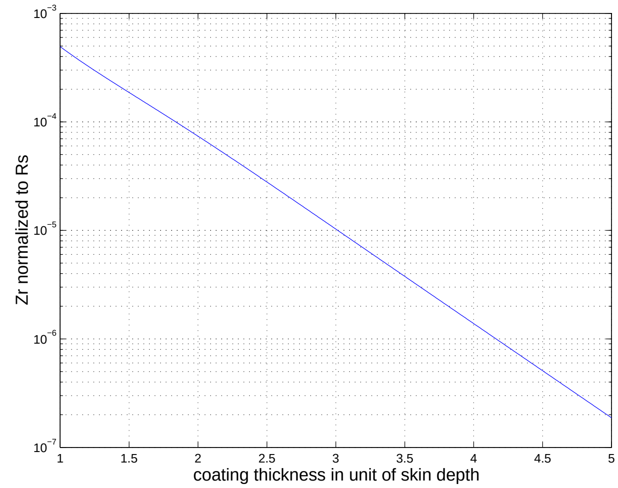

Fig. 5. Radiation impedance R_r of a thin metal film as a function of film thickness. Substrate is dielectric with $\epsilon_{3r} = 5.5$.

of current in the metal film with $\Delta r = \frac{1}{2}\pi\delta_2$. The amplitude is normalized to the surface value of an infinite thick metal. Notice that the phase lagging is within 90^o, so there is no reverse current. And the electric field on the thin film surface is smaller than that of the infinite thick metal.

III. Radiation Impedance

The RF leakage through the metal film, characterized by the power radiated to media 3 per unit area, can be expressed as

$$P_r = \frac{1}{2}Re(E_z * H_\phi^*)|_{r=r_2} = \frac{1}{2}Re(\frac{|E_z|^2}{Z_2})|_{r=r_2}. \quad (17)$$

If we define a transfer impedance Z_t to relate the electric field E_z at $r = r_2$ to the surface magnetic field H_ϕ at $r = r_1$ as

$$Z_t \equiv \frac{E_z|_{r=r_2}}{H_\phi|_{r=r_1}} = \frac{Z_2}{\cos k_{2r}\Delta r - i(Z_2/Z_{2c})\sin k_{2r}\Delta r}, \quad (18)$$

then the power leakage becomes

$$P_r = \frac{1}{2}Re(\frac{|Z_t|^2}{Z_2})|H_\phi|^2|_{r=r_1} \equiv \frac{1}{2}R_r|H_\phi|^2|_{r=r_1}, \quad (19)$$

where we define radiation impedance R_r so we can compare to surface impedance Z_1, whose real part indicates total power loss. In the case that $|k_{2r}\Delta r| > 1$, we can further simplify

$$R_r = Re(\frac{|Z_t|^2}{Z_2}) = R_s\frac{8R_s}{|Z_{3c}|}e^{-2\Delta r/\delta_2}. \quad (20)$$

The numerical value of R_r is plotted in Fig. 5. The exponential dependence of R_r on the large film thickness Δr is obvious. But even with a film 1.5 skin depth thick, radiation into media 3 only amounts to 2×10^{-4} that of the total power loss. This is a result of near total reflection at the interface between media 2 and 3 due to the large difference between the characteristic impedance Z_{2c} and Z_{3c}. The reflection coefficient from media 2 to 3,

$$r_{23} = \frac{Z_{3c} - Z_{2c}}{Z_{3c} + Z_{2c}} \quad (21)$$

is nearly one. Thus the fractional power transmitted through the interface is

$$1 - |r_{23}|^2 = \frac{4R_s}{|Z_{3c}|}. \quad (22)$$

If we include the attenuation in the metal film we would have

$$\frac{R_r}{R_s} = \frac{4R_s}{|Z_{3c}|}e^{-2\Delta r/\delta_2}. \quad (23)$$

The difference between Eq. 20 and 23 is a result of the non unitarity of the S-matrix when a mode with complex impedance is present[7].

IV. Multi-layer Coatings

The results in the previous sections can be generalized to multi-layer coatings through repeated use of Eq. 11 and 18. A n-layer coatings system is defined by a one-dimensional array r_j, j from 1 to $n-1$, which specifies the interface coordinate between medium j and $j+1$. We have

$$Z_{j-1} \equiv \frac{E_z}{H_\phi}|_{r=r_{j-1}} = Z_{jc}\frac{(Z_j/Z_{jc})\cos\phi_j - i\sin\phi_j}{\cos\phi_j - i(Z_j/Z_{jc})\sin\phi_j} \quad (24)$$

$$Z_{tj} \equiv \frac{E_z|_{r=r_{j+1}}}{H_\phi|_{r=r_j}} = \frac{Z_{j+1}}{\cos\phi_j - i(Z_j/Z_{jc})\sin\phi_j} \quad ,(25)$$

where

$$\phi_j = k_{jr}(r_{j+1} - r_j) \quad (26)$$

$$Z_{jc} = \frac{k_{jr}}{\omega\epsilon_j(1 + i\sigma_j/\omega\epsilon_j)} \quad (27)$$

$$k_{jr} = \sqrt{\omega^2\mu_j\epsilon_j(1 + i\sigma_j/\omega\epsilon_j) - k_z^2} \quad (28)$$

and outgoing wave boundary condition

$$Z_{n-1} = Z_{nc}. \tag{29}$$

Then we obtain the transfer impedance from $r = r_1$ to $r = r_{n-1}$

$$Z_t = \frac{\prod_{j=1}^{n-2} Z_{tj}}{\prod_{j=2}^{n-2} Z_j} = \frac{Z_{t(n-1)}}{\prod_{j=2}^{n-2} [\cos\phi_j - i(Z_j/Z_{jc})\sin\phi_j]} \tag{30}$$

and the radiation impedance

$$R_r = \Re\frac{|Z_t|^2}{Z_{nc}}. \tag{31}$$

Taking the PEP-II B-factory[8] as an example, the IR chamber inside the detector is a 40 cm long double-wall beryllium pipe. The walls are 0.8 mm and 0.4 mm thick respectively with 1 mm gap for cooling water. The ID of the wall is 5 cm. Even though the beryllium walls represent less than 5 skin depths at 136 kHz revolution frequency, the radiated power into the detector by a 3 A beam with 5% gap is only 1×10^{-13} watts.

V. Beam Impedance

In addition to confining RF power, metal enclosures are also used to transport charged beams. An important figure of merit is the beam impedance defined as

$$Z_b(\omega) = \frac{\int_0^L E_z(\omega, z) e^{-i\omega z/v} dz}{I_b(\omega)}, \tag{32}$$

where v is the speed of the charged beam. For a long beam pipe, E_z is proportional to $e^{i\omega z/v}$, thus

$$Z_b = \frac{E_z L}{I_b} = \frac{Z_1 H_{1\phi}}{I_b} L = Z_1 \frac{L}{2\pi r_1}, \tag{33}$$

where we have used the fact that E_z is uniform inside region 1 for highly relativistic beam and also $H_{1\phi} = I_b/2\pi r_1$. Because Z_b is the same as the surface impedance Z_1 aside from a geometric factor, we will continue using Z_1 when we refer to beam impedance.

A. Impedance spectrum

A bunched beam with length σ_b has frequency contents up to $\omega_b = c/\sigma_b$, and this sets a natural frequency reference. A reference for metal thickness is provided by the skin depth

$$\delta_b = \sqrt{\frac{2}{\omega_b \mu_0 \sigma_2}} \tag{34}$$

at ω_b. With a beam of $\sigma_b = 1$ cm, the frequency range $\omega_b/2\pi = 4.77$ GHz and $\delta_b = 0.96$ μm in copper.

Beam impedance is readily available from Eq. 11, and plotted in Fig. 6. We have chosen $\epsilon_{3r} = 5.5$, copper film and $\sigma_b = 1$ cm. The metal film thickness is specified in unit of the skin depth δ_b. The thick coating limit exhibits a normal square root dependence on frequency. When the coating becomes thinner, the fields inside metal become gradually

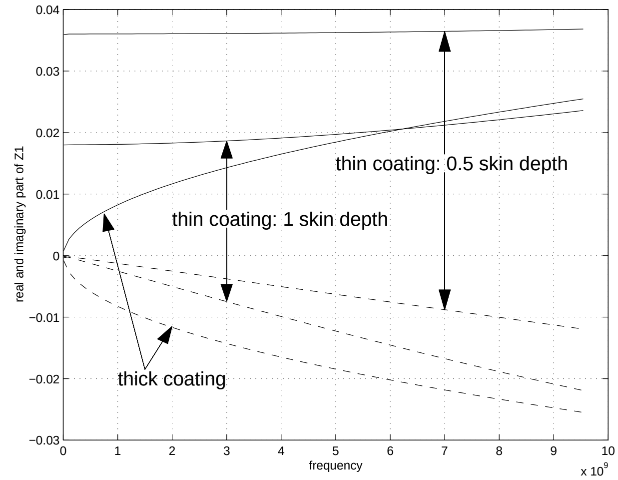

Fig. 6. The beam impedance as a function of frequency. The solid and dashed lines represent real and imaginary part of the impedance respectively. The bunch length σ_b is chosen to be 1 cm.

more uniform. The resistance, i.e., the real part of the impedance, therefore approaches the DC limit, $1/\sigma\Delta r$. As a result, the resistance becomes less frequency dependent. This scaling eventually breaks down when Eq. 15 does not hold. Then the metal film becomes too thin to shield the RF field, i.e., when it can not conduct all the image current. At the limit of zero metal thickness, the resistance of metal goes to zero.

While resistance is increased across most of the spectrum with a thinner coating, the reactance, i.e., the imaginary part of the impedance, predominately inductive, is reduced as a result of less volume in the metal to store magnetic energy.

The results can be understood qualitatively by expanding Eq. 13 to obtain

$$Z_1 = \frac{1}{\sigma_2 \Delta r}[1 + \frac{4}{45}(\frac{\Delta r}{\delta_2})^4] - i\omega\frac{\mu_0 \Delta r}{3}, \tag{35}$$

where we have used the Taylor expansion

$$\frac{x}{\tan x} = 1 - \frac{1}{3}x^2 - \frac{1}{45}x^4 + O(x^6). \tag{36}$$

Just as we observed in Fig. 6, the resistance is inversely proportional to Δr at DC and has a quadratic increase with frequency because $\delta_2 \propto 1/\sqrt{\omega}$, while inductance is proportional to Δr.

If material 3 is another metal, Eq. 11 reduces to

$$Z_1 = \frac{1}{\sigma_2 \Delta r} \frac{\cos x - i\beta \sin x}{\sin x + i\beta \cos x} x, \tag{37}$$

where $\beta = \sqrt{\sigma_3/\sigma_2}$ and $x = (1+i)\Delta r/\delta_2$. Fig. 7 illustrates the beam spectrum of a 1 cm bunch, with $\sigma_3/\sigma_2 = 0.02$. At low frequency, the RF fields penetrate through metal 2, and the impedance follows that of metal 3. When penetration depth becomes comparable to the coating thickness at high frequency, the impedance approaches that of metal

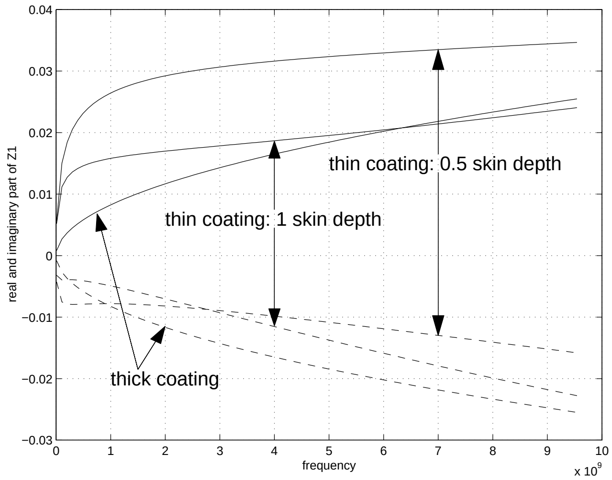

Fig. 7. The beam impedance as a function of frequency. The solid and dashed lines represent real and imaginary part of the impedance respectively. The bunch length σ_b is chosen to be 1 cm.

2. In the transition frequency range, the impedance has a less frequency dependent resistance and inductance. The smaller the β, the faster the initial rise, and a closer resemblance to Fig. 6.

B. Effective Impedance

One way to quantify the effect of impedance on a beam is the beam spectrum weighted impedance average. Thus we define quantity

$$k = 2\int_0^\infty \Re(Z_b(\omega))|I(\omega)|^2\frac{d\omega}{2\pi}, \tag{38}$$

which gives energy loss. We do not need to take the real part when integrating from $-\infty$ to ∞ because $\Im(Z_b)$ is an odd function of ω. For a Gaussian bunch profile

$$\rho(s) = \frac{q}{\sqrt{2\pi}\sigma_b}e^{-s^2/2\sigma_b^2}, \tag{39}$$

the current spectrum is also Gaussian

$$I(\omega) = qe^{-(\omega/c)^2\sigma_b^2/2}. \tag{40}$$

Substituting Eq. 33 and 40 into 38, we obtain

$$k = \frac{L}{2\pi r_1}2\int_0^\infty \Re(Z_1)q^2e^{-(\omega/c)^2\sigma_b^2}\frac{d\omega}{2\pi}. \tag{41}$$

If the thick metal Z_1 is used, we obtain the familiar result

$$k_{thick} = \frac{L}{2\pi r_1}\frac{cq^2}{\sigma_b}\sqrt{\frac{Z_0}{2\sigma\sigma_b}}\frac{\Gamma(\frac{3}{4})}{2\pi}, \tag{42}$$

where we applied the definition of Gamma function

$$\Gamma(z) = \int_0^\infty y^{z-1}e^{-y}dy. \tag{43}$$

By substituting Eq. 13 or 37 in Eq. 41 for thin metal coating, we have

$$k_{thin} = \frac{L}{2\pi r_1}\frac{cq^2}{\sigma_b}\sqrt{\frac{Z_0}{2\sigma\sigma_b}}\frac{\Gamma(\frac{3}{4})}{2\pi}\alpha_Z \tag{44}$$

with

$$\alpha_Z = \Re[\frac{1+i}{\Gamma(\frac{3}{4})}\int_0^\infty \frac{y^{-1/4}e^{-y}}{\tan x}dy] \tag{45}$$

for metal coating on dielectric and

$$\alpha_Z = \Re[\frac{1+i}{\Gamma(\frac{3}{4})}\int_0^\infty \frac{\cos x - i\beta\sin x}{\sin x + i\beta\cos x}y^{-1/4}e^{-y}dy] \tag{46}$$

for metal film on metal. We have defined $\beta = \sqrt{\sigma_3/\sigma_2}$ and $x = (1+i)(\Delta r/\delta_b)y^{-1/4}$.

Another figure of merit that enters directly into the beam instability is the averaged Z_b/ω[9]

$$(\frac{Z_b}{\omega})_{eff} = \frac{\sum_{p=-\infty}^{\infty} Z_b(\omega')/\omega' h_l(\omega')}{\sum_{p=-\infty}^{\infty} h_l(\omega')}, \tag{47}$$

where

$$h_l(\omega) = (\frac{\omega\sigma_b}{c})^{2l}e^{-(\omega/c)^2\sigma_b^2}, \tag{48}$$

and

$$\omega' = p\omega_0 + l\omega_s. \tag{49}$$

The quantities ω_0 and ω_s are revolution and synchrotron frequencies respectively. For broad band impedance, we can replace the sum by an integral, and the real part vanishes because $\mathrm{Re}(Z_b)$ is an even function of ω. The vanishing result holds true in the limit $\omega_s \to 0$.

Substituting the metal surface impedance into Eq. 47, we obtain

$$(\frac{Z_b}{\omega})_{eff} = -i\frac{L}{2\pi r_1}\frac{\sqrt{\frac{Z_0}{2\sigma\sigma_b}}}{\omega_b}\frac{\Gamma(l+\frac{1}{4})}{\Gamma(l+\frac{1}{2})}. \tag{50}$$

Similarly, the effective impedance of thin metal coating is

$$(\frac{Z_b}{\omega})_{eff} = -i\frac{L}{2\pi r_1}\frac{\sqrt{\frac{Z_0}{2\sigma\sigma_b}}}{\omega_b}\frac{\Gamma(l+\frac{1}{4})}{\Gamma(l+\frac{1}{2})}\alpha_{\frac{Z}{\omega},l} \tag{51}$$

with

$$\alpha_{\frac{Z}{\omega},l} = \Im[\frac{-(1+i)}{\Gamma(l+\frac{1}{4})}\int_0^\infty \frac{y^{l-\frac{3}{4}}e^{-y}}{\tan x}dy] \tag{52}$$

for metal on dielectric and

$$\alpha_{\frac{Z}{\omega},l} = \Im[\frac{-(1-i)}{\Gamma(l+\frac{1}{4})}\int_0^\infty \frac{\cos x - i\beta\sin x}{\beta\cos x - i\sin x}y^{l-\frac{3}{4}}e^{-y}dy] \tag{53}$$

for metal on metal.

The value of α's are plotted in Fig. 8. In order to fit the lines in the same range, we plot $1/\alpha_Z$ and $\alpha_{\frac{Z}{\omega},1}$. The value of α_Z generally scales as $1/\Delta r$ and $\alpha_{\frac{Z}{\omega},1}$ is proportional to Δr at small Δr, which is the result of Eq. 35. The $\alpha_{\frac{Z}{\omega},1}$ of metal film on metal increases at smaller Δr value because of the field penetration. For metal film on dielectric,

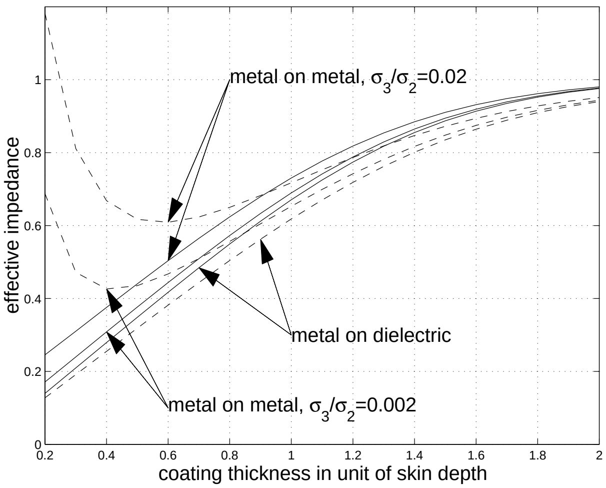

Fig. 8. The effective impedance plotted as a function of coating thickness. The solid lines are $1/\alpha_Z$ and dashed lines are $\alpha_{\frac{Z}{\omega},1}$.

α_Z and $\alpha_{\frac{Z}{\omega},1}$ can be traded against each other with their product roughly constant. For metal film on metal, the minimum $\alpha_{\frac{Z}{\omega},1}$ is 0.61 and 0.43 for $\sigma_3/\sigma_2 = 0.02$ and 0.002 respectively. The corresponding energy loss is 2 and 3.2 times more.

Since dipole impedance is also proportional to surface impedance Z_1, it follows the same analysis as longitudinal impedance.

VI. Conclusions

We have derived the RF and beam impedance of a thin metal coating. The surface impedance can be reduced by 8% if metal thickness of about $\frac{1}{2}\pi\delta$ is chosen; this reduction results from eliminating reverse current flow. The RF leakage through thin metal film is very small due to the large mismatch of impedance. It is then possible to attach a high thermal conductivity material, like diamond, to the back of the metal film to facilitate cooling.

The beam impedance of thin metal film is also derived. For a thin coating, it is found to have a rather smooth resistance spectrum. The reduced inductance at smaller coating thickness may be useful in reducing bunch lengthen in high current storage ring where resistive wall contribution is relatively large[10]. A copper coating of $0.6\delta_b$ thick on stainless steel reduces the inductance by 39% compared with thick copper wall.

Acknowledgments

The authors would like to acknowledge helpful discussions with Dr. Norman Kroll.

References

[1] A. Piwinski, "Penetration of the field of a bunched beam through a ceramic vacuum chamber with metallic coating", *IEEE transactions on Nuclear Science*, Vol 24, No.3, June 1977, pp. 1364-1366.
[2] A. W. Chao, *Physics of Collective Beam Instabilities in High Energy Accelerators.* New York: Wiley, 1993. pp. 71.
[3] J. D. Jackson, SSC-N-110. 1986. Unpublished.
[4] E. D. Courant and M. Month, "Transverse resistive wall instability of an off-axis ribbon beam in a circular chamber", BNL Report BNL-50875, 1978. Unpublished
[5] J. D. Jackson, *Classical Electrodynamics.* 2nd ed., New Work: Wiley, 1975, pp. 334-339.
[6] D. R. Lide, *Handbook of chemistry and physics.* 77th ed., CRC press, 1997, pp. 6-200.
[7] Xintian E. Lin, *Transverse Wakefield of Waveguide Damped Structures and Beam Dynamics*, Ph.D. thesis, SLAC-R-472, pp. 95-102.
[8] *PEP-II An Asymmetric B-factory, Conceptual Design Report*, SLAC-418, 1993. Unpublished
[9] A. W. Chao, *Physics of Collective Beam Instabilities in High Energy Accelerators.* New York: Wiley, 1993. pp. 320.
[10] S. Heifets *et al.* "Impedance study for the PEP-II B-factory" SLAC/AP-99. Unpublished

Xintian E. Lin was born in Chengdu, China, in 1969. He received the B.Sc degree in physics from the University of Science and Technology of China in 1988. He subsequently attended University of California, San Diego, and received the Ph.D. in physics in 1995. From 1995 to 1997, he worked as research physicist on the SLAC B-factory RF design. Since 1997, he is with Accelerator Research Department. His research interest is in diamond coating and design of high gradient accelerator structures, wakefield of waveguide damped cavities and beam dynamics.